Letter

Dissipative drift instability of plasmons in a single-layer graphene

I. M. Moiseenko [1,2,*] D. V. Fateev [1,3] and V. V. Popov [1]

[1]*Kotelnikov Institute of Radio Engineering and Electronics (Saratov Branch), Russian Academy of Sciences, Saratov 410019, Russia*

[2]*Center for Photonics and 2D Materials, Moscow Institute of Physics and Technology (National Research University), Dolgoprudny 141700, Russia*

[3]*Saratov State University, Saratov 410012, Russia*

(Received 11 May 2023; accepted 28 November 2023; published 3 January 2024)

We predict the plasmon instability associated with losses in hydrodynamic graphene with a drift-current bias. The instability appears even in a single-layer graphene and becomes stronger for greater losses in graphene in hydrodynamic regime but disappears in the lossless case. The unstable plasmon mode vanishes for zero drift velocity instead of transforming into any plasmon mode existing in graphene without carrier drift. The dissipative instability occurs for any finite drift velocity but the instability increment decreases down to zero for vanishing carrier drift velocity. The strongest instability develops for codirected carrier drift and plasmon propagation directions.

DOI: 10.1103/PhysRevB.109.L041401

Physical properties of a material system dramatically depend on its dimensionality [1]. Plasma oscillations (plasmons) in two-dimensional (2D) electron systems have been studied since almost half a century ago [2–6]. It is remarkable that plasmons in a 2D electron system are dispersive waves even in a long-wavelength limit in distinction from plasma oscillations in 3D plasma. It means that 2D plasmons have nonzero group velocity and hence can transmit electromagnetic signals, which opens the way to their practical applications for information processing. In the beginning of the 21st century, graphene, the ultimately thin (one-atom thick) 2D flatland material, was discovered [7,8]. Since then a variety of different 2D materials have been synthesized and investigated [9]. Due to the Dirac (linear) energy spectrum of massless carriers in graphene, the dispersion of plasmons in graphene (also termed as the Dirac plasmons) is too much different from that for plasmons in 2D electron systems with massive carriers [10–12]. Graphene plasmonics has been a source of amazing and extraordinary discoveries in recent years, and also paved a way to new, promising practical applications in terahertz (THz) frequency range [13]. Graphene, due to its unique physical and performance properties, is actively being investigated as an element of compact detectors [14,15], amplifiers [16,17], and a variety of other THz devices [18,19].

The motion of charge carriers in graphene can be described by hydrodynamic theory at THz frequencies, when the rate of carrier-carrier collisions is greater than the rate of carrier collisions with impurities and phonons in graphene and greater than the frequency of exerted electric field [20–24]. Experimental confirmation of the hydrodynamic behavior of charge carriers in graphene was reported in Refs. [25–27]. Hydrodynamic regime typically sets in for temperatures $T > 30$–100 K depending on the carrier density in graphene [27]. At such temperatures, the carrier-carrier scattering rate is about $\gamma_{ee} \geqslant 5 \times 10^{12}$ s^{-1} at the hydrodynamic regime onset and grows as $\gamma_{ee} \sim T^2$ for higher temperatures [27]. It means that the hydrodynamic regime can take place in the low part of THz frequency range $\omega < \gamma_{ee}$ ($\omega/2\pi \leqslant 5$ THz) up to room temperature. Another important requirement that should be fulfilled in the hydrodynamic regime is the inequality $\gamma < \gamma_{ee}$, where γ is the rate of carrier momentum relaxation due to disorder and phonons. The carrier momentum relaxation rate can be as low as $\gamma \simeq 2 \times 10^{12}$ s^{-1} in graphene with high carrier mobility up to room temperature [28,29]; hence, the inequality $\gamma < \gamma_{ee}$ can be fulfilled. In the hydrodynamic regime, graphene behaves as a fluid and demonstrates interesting properties absent in the ballistic regime $\gamma, \gamma_{ee} \ll \omega$ [27,30]. Hydrodynamic graphene supports the transverse-magnetic (TM) plasmons with phase velocity $V_{\rm ph} > V_{\rm F}/\sqrt{2}$ [23,31,32], where $V_{\rm F} = 10^6$ m/s is the Fermi velocity in graphene [33,34], while in the ballistic regime, the plasmon velocity in graphene cannot be below $V_{\rm F}$ [23,35].

Carrier drift makes graphene anisotropic and leads to the effects of graphene birefringence and nonreciprocal Doppler shift of Dirac plasmons [36–42]. The nonreciprocal Doppler shift of Dirac plasmons in graphene with carrier drift bias was experimentally observed in Refs. [43,44]. It was claimed in Refs. [45,46] that the plasmon instability in bilayer graphene with charge-carrier drift in the ballistic regime is possible due to negative Landau damping for low phase velocity of plasmons $V_{\rm ph} < V_0$ (Cherenkov instability condition), where V_0 is the drift velocity of charge carriers in graphene. However, as it was later argued in Refs. [47,48], the Cherenkov instability in graphene bilayer can take place only in the hydrodynamic regime and it is prohibited in the ballistic regime. Remarkably, the Cherenkov instability develops even in the absence of dissipative collisions in graphene and it is prohibited in a

*MoiseenkoIM@yandex.ru

single-layer graphene [45,49]. It is known however that a non-Cherenkov plasmon instability can develop due to negative Landau damping in the ballistic (collisionless) regime even in a single-layer 2D electron system with massive charge carriers as a result of the effect of the stationary electric field on high-frequency electron dynamics [50]. The drift-induced plasmon instabilities associated with material absorption (dissipative instabilities) were predicted for 2D electron systems with massive charge carriers [51,52]. However, those instabilities exist only in two coupled plasmonic systems (with carrier drift at least in one of those) but not in a single-layer 2D electron system. The experimental work [53] demonstrates the possibility of drift-induced non-Cherenkov amplification of THz plasmons in a graphene transistor structure with a grating gate.

In this paper, we predict the existence of a slow plasmon mode in a single-layer graphene with a drift-current bias in the hydrodynamic regime. The mode disappears for zero carrier drift instead of transforming into any plasmon mode existing in graphene without carrier drift. We show that this mode becomes unstable in lossy graphene. The instability develops exclusively due to losses in graphene and it disappears in a lossless case. Remarkably, the dissipative instability occurs for any finite drift velocity though the instability increment decreases down to zero for vanishing carrier drift velocity. The strongest instability develops for codirected carrier drift and plasmon wave vector. We show that the instability increment decreases for oblique angles between carrier drift and plasmon propagation directions so that the unstable mode becomes damped for angular deflection between those directions greater than 45° and finally this mode disappears in the case of transversal drift. To discover this type of the plasmon instability, we extend the hydrodynamic theory elaborated in Refs. [20–24] by taking into account the effect of static biasing (drift-inducing) electric field on the oscillating hydrodynamic variables.

The studied structure consists of a graphene sheet located in the plane x-z between two semi-infinite dielectric materials with dielectric constants ε_1 and ε_2. All calculations are performed for the structure with $\varepsilon_1 = \varepsilon_2 = \varepsilon_b = 4.5$ (boron nitride) [54]. We will consider plasmons propagating along the x axis in graphene with the spatiotemporal dependence of plasmon fields $\propto \exp(-i\omega t + ik_x x)$, where ω is the angular frequency and k_x is the plasmon longitudinal wave vector, and we assume that the constant carrier drift current flows at arbitrary angle to the plasmon propagation direction.

Graphene with the stationary carrier drift is generally described by the 2D conductivity tensor $\hat{\boldsymbol{\sigma}}$. Elements of the graphene hydrodynamic conductivity tensor are obtained by solving the continuity equation, the charge-carrier momentum balance equation, and the energy balance equation for 2D motion of charge carriers in graphene [20–24]:

$$\frac{\partial N}{\partial t} + \frac{\partial (N\mathbf{V})}{\partial x} = 0, \tag{1}$$

$$\frac{\partial \mathbf{S}}{\partial t} + \nabla \cdot \widehat{\mathbf{\Pi}} + e\mathbf{E}N = -\gamma \mathbf{S}, \tag{2}$$

$$\frac{\partial W}{\partial t} + V_F^2 \nabla \cdot \mathbf{S} + eN\mathbf{E} \cdot \mathbf{V} = 0, \tag{3}$$

where N is the charge-carrier density, $\mathbf{V}$ is the hydrodynamic velocity, $\mathbf{S}$ is the macroscopic momentum density, W is the macroscopic energy density, $\widehat{\mathbf{\Pi}}$ is the momentum flux tensor (sometimes termed as the stress-energy tensor or energy-momentum tensor) [20], e is the elementary charge ($e > 0$), $\mathbf{E}$ is the in-plane electric field, $\gamma = 1/\tau$, with τ being the momentum relaxation time of charge carriers in graphene. The relations between the physical quantities entered Eqs. (1)–(3) can be written as [20,55]

$$\mathbf{S} = M\mathbf{V}, \quad W = MV_F^2 - P, \quad P = M\left(V_F^2 - \mathbf{V}^2\right)/3,$$
$$\widehat{\mathbf{\Pi}} = P\hat{\mathbf{I}} + \mathbf{S} \otimes \mathbf{V}, \tag{4}$$

where M is the hydrodynamic mass density, P is the hydrodynamic pressure, and $\hat{\mathbf{I}}$ is the unit tensor.

By linearizing the hydrodynamic equations (1)–(3) in respect to the oscillating hydrodynamic variables around the stationary drift state (see the Supplemental Material to Ref. [55]), we obtain the expressions for each element of the linear conductivity tensor of graphene with a constant carrier drift taking into account the effect of static drift-inducing electric field on the oscillating hydrodynamic variables. The conductivity demonstrates the spatial dispersion and depends on the frequency ω, plasmon longitudinal wave vector k_x, drift velocity V_0, and the steady-state Fermi energy ε_F in graphene. In contrast to 2D electron systems with massive carriers, the graphene conductivity depends on drift velocity even in the absence of spatial dispersion in the long-wavelength limit (for zero wave vector), which is the consequence of breaking the Galilean invariance in graphene with massless carriers [24]. The explicit expressions for elements of the graphene conductivity tensor are too much bulky in the case of oblique carrier drift (even in the simplest case of collinear carrier drift and plasmon propagation directions, the expression for governing element σ_{xx} of the graphene conductivity tensor is quite lengthy [55]). However, it is crucially important that the carrier momentum relaxation rate $\gamma > 0$ is involved as a prefactor in the real part of every element of the graphene conductivity tensor. Though the rest of factors in the elements of the conductivity tensor also contain the carrier momentum relaxation rate, the real parts of some tensor elements can be nevertheless negative for certain drift velocities, giving rise to the plasmon instability. However, the instability disappears when $\gamma = 0$ for any drift velocity value. Therefore, this type of instability is a dissipative one by its very nature.

In general, all elements of the graphene conductivity tensor enter the dispersion equation for surface waves in graphene propagating along the x axis [56]:

$$\left[\omega\varepsilon_0\left(\frac{\varepsilon_1}{k_{y1}} - \frac{\varepsilon_2}{k_{y2}}\right) + \sigma_{xx}\right](k_{y2} - k_{y1} - \sigma_{zz}\mu_0\omega) = -\sigma_{xz}\sigma_{zx}\mu_0\omega, \tag{5}$$

where $k_{y1,2} = \pm\sqrt{\omega^2\varepsilon_{1,2}/c^2 - k_x^2}$ are the normal-to-plane-of-graphene components of the plasmon wave vectors in different media, c is the speed of light, ε_0 and μ_0 are the electric and magnetic constants, respectively. The signs of $k_{y1,2}$ are chosen in order to correspond with the exponential decay of the plasmon field away from the graphene layer. We assume the

frequency to be a real quantity and seek for complex solutions for the plasmon wave vector.

When the direction of charge-carrier drift coincides with (or opposite to) the direction of plasmon propagation ($V_{z0} = 0$, $V_{x0} \neq 0$), the condition $\sigma_{zx} = \sigma_{xz} = 0$ is valid and dispersion relation (5) splits into two equations:

$$k_{y2} - k_{y1} - \sigma_{zz}\mu_0\omega = 0, \quad \text{and} \tag{6}$$

$$\omega\varepsilon_0\left(\frac{\varepsilon_1}{k_{y1}} - \frac{\varepsilon_2}{k_{y2}}\right) + \sigma_{xx} = 0. \tag{7}$$

Equation (6) describes the transverse-electric (TE) modes and it has no solution in the form of surface wave for $V_{z0} = 0$ because, in this case, the graphene conductivity σ_{zz} exhibits the inductive nature ($\mathrm{Im}\sigma_{zz} > 0$) in a low part of THz frequency range, which does not satisfy the condition of existence of the surface TE modes in graphene [57]. However, Eq. (6) can have solution for the surface TE modes in a low part of THz frequency range if the direction of carrier drift is transverse to the TE wave propagation direction and V_{z0} exceeds a threshold value as shown in Refs. [56,58]. We do not consider TE modes in this paper because these modes were studied in Refs. [56,58] in detail.

In this paper, we focus on exploring Eq. (7), which describes the dispersion of surface TM plasmons (more exactly, plasmon-polaritons). We found two different surface plasmon modes with TM polarization existing in graphene for codirected carrier drift and plasmon wave vector ($\mathrm{Re}k_x > 0, V_{x0} > 0$). The dispersions of these modes are shown in Figs. 1(a) and 2 by solid lines for different drift velocities of charge carriers in graphene. One of the modes is attenuated ($\mathrm{Im}k_x > 0$), and the other is amplified ($\mathrm{Im}k_x < 0$) for all studied THz frequencies. To be concise, we will term the mode with $\mathrm{Im}k_x > 0$ as the "damped mode," and the mode with $\mathrm{Im}k_x < 0$ as "amplified mode."

Let us start with considering the damped mode. For $V_0 = 0$, this mode is the well-known surface TM plasmon in graphene. For each finite value of the drift velocity V_{x0} there is a cutoff frequency below which there are no damped TM modes. This is due to the capacitive nature of graphene conductivity ($\mathrm{Im}\sigma_{xx} < 0$) below these frequencies [see the dashed lines in Fig. 1(a)], which does not satisfy the condition of the surface TM plasmon mode existence [57]. The real part of the graphene conductivity $\mathrm{Re}\sigma_{xx}$ is positive for the damped mode and grows with increasing V_{x0} at a fixed frequency, which leads to an increase in the attenuation of this mode [see Fig. 1(b)]. The cutoff frequency decreases with decreasing V_{x0} and becomes zero for $V_{x0} = 0$. With the losses taken into account, all dispersion curves enter the fast-wave region ($\mathrm{Re}k_x < \omega\sqrt{\varepsilon_b}/c$) in Fig. 1(a), although the TM modes remain surface waves. In this region, the surface TM modes suffer from strong damping [overdamped plasmon segments of the attenuation curves, where the inequality $\mathrm{Im}k_x/\mathrm{Re}k_x > 1$ is valid, are shown by dashed lines in Fig. 1(b)]. In the lossless case, the surface TM mode exists totally in the slow-wave region ($\mathrm{Re}k_x > \omega\sqrt{\varepsilon_b}/c$) for any drift velocity without cutoff. A similar damped surface TM mode (not shown in the figures) exists for counterdirected carrier drift and plasmon wave vector ($V_{x0} > 0, \mathrm{Re}k_x < 0$). It differs only slightly from the damped mode codirected with the carrier drift, which is considered above, due to the insignificant effect of the Doppler shift for these modes ($|\mathrm{Re}k_x| \ll \omega/V_{x0}$). The difference between the wavelengths of damped plasmon modes

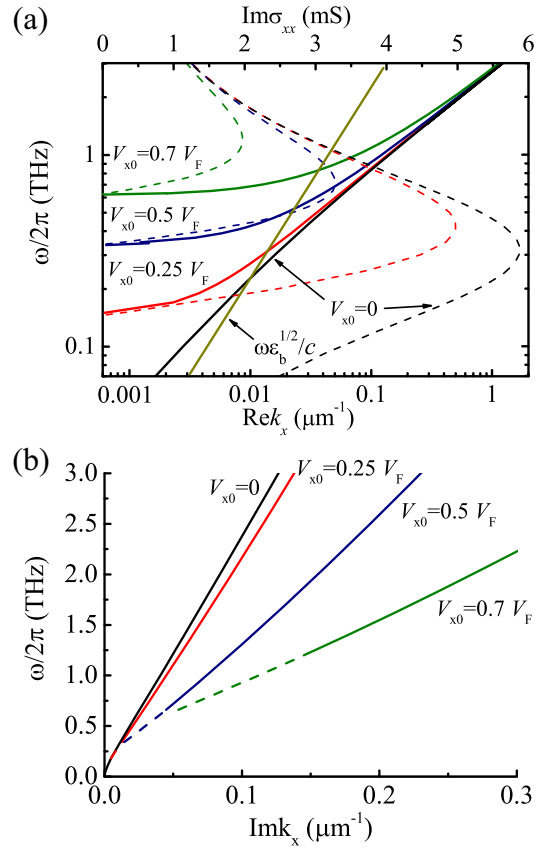

FIG. 1. (a) The real and (b) imaginary parts of the longitudinal wave vector of the damped plasmon mode as functions of frequency for codirected carrier drift and plasmon longitudinal wave vector for different values of V_{x0}. The imaginary part of graphene conductivity is shown in panel (a) by dashed lines (top horizontal axis). The segments of the plasmon increment curves, where the inequality $\mathrm{Im}k_x/\mathrm{Re}k_x > 1$ is valid, are shown by dashed lines in panel (b). Graphene parameters are $\varepsilon_F = 200$ meV and $\tau = 0.5$ ps.

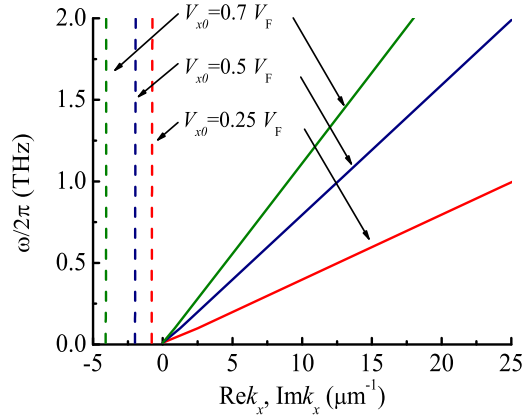

FIG. 2. The real (solid curves) and imaginary (dashed curves) parts of the plasmon longitudinal wave vector for the amplified plasmon mode propagating downstream of the carrier drift. Graphene parameters are $\varepsilon_F = 200$ meV and $\tau = 0.5$ ps.

propagating downstream and upstream of the carrier drift does not exceed 5% in the entire range of THz frequencies. This result is in good agreement with the experimental data reported in Refs. [43,44]. It is worth noting that in Refs. [43,44] as well as in theoretical papers [36–42], the effect of drift current on the plasmon modes already existing in graphene even without carrier drift is studied only.

The damped mode exists at any oblique drift angle even when the carrier drift is strictly perpendicular to the plasmon propagation direction. The attenuation of this mode decreases with increasing the angle between the carrier drift and the plasmon propagation directions. The decrease of plasmon damping for oblique drift is due to decreasing the component of drift velocity V_{x0}. In the case of carrier drift perpendicular to the plasmon wave vector the attenuation decreases at least by a factor of 2 compared to the attenuation of plasmons in the case of collinear drift and the plasmon propagation directions. For $V_{z0} = 0.7V_{\mathrm{F}}$ and $V_{x0} = 0$, the damping of the plasmon mode decreases by at least 40% in the entire frequency range under study as compared with the plasmon mode in the absence of electron drift in graphene.

Now we consider the surface TM plasmon which does not exist in any form in graphene without carrier drift. Figure 2 shows the real and imaginary parts of the plasmon longitudinal wave vector of the amplified TM plasmon mode for codirected carrier drift and plasmon propagation directions. The phase velocity of amplified plasmon mode ($V_{\mathrm{ph}} = \omega/\mathrm{Re}k_x$) is close to the carrier drift velocity so that the value of $\mathrm{Re}k_x$ decreases with growing drift velocity for a given frequency. This behavior is typical for dissipative instabilities in 2D electron systems with massive charge carriers [51,52]. The imaginary part of the plasmon wave vector is negative at THz frequencies for any finite drift velocity value, which indicates the amplification (instability) of this mode along the propagation direction. Amplification takes place due to the fact that the real part of the graphene conductivity is negative $\mathrm{Re}\sigma_{xx} < 0$ for all frequencies and wave vectors of this mode. The increment of amplified mode tends to zero for $V_{x0} \to 0$, and its dispersion curve merges with the abscissa axis in Fig. 2 so that the mode frequency is equal to zero for all wave vectors in this case. The increment of the amplified plasmon mode is almost independent of the real part of the plasmon wave vector (see Fig. 2) which is also consistent with the characteristic features of dissipative plasmon instabilities in 2D electron systems with massive carriers [51,52]. The increment of the amplified mode vanishes in the lossless case (when $\gamma = 0$) while its dispersion remains almost independent of losses if the inequality $|\mathrm{Re}k_x/\mathrm{Im}k_x| > 1$ is satisfied. Remarkably, the amplification increment increases with growing losses in graphene for any fixed drift velocity within the hydrodynamic regime. We have not found an amplified mode propagating upstream of the carrier drift for the studied frequencies and drift velocities.

In the case of oblique carrier drift, the tensor nature of the graphene conductivity leads to the excitation of in-plane component of the plasmon electric field E_z and additional components of magnetic field H_x and H_y. Therefore, the plasmons are the hybrid TM+TE modes in this case and one has to solve the general dispersion relation (5) which involves all elements of the graphene conductivity tensor instead of using the dispersion relation (7) for TM modes. The calculations show that the increment of the amplified mode decreases with increasing the angle α between the carrier drift and plasmon propagation directions. The amplification turns into attenuation for $\alpha > 45^\circ$, and finally this mode disappears in the case of transversal drift $\alpha = 90^\circ$.

Since the amplified mode is very slow (its phase velocity is by two orders of magnitude smaller than the speed of light), the spatial dispersion in graphene totally determines the properties of this mode and even is the cause of its very existence. That is why such mode did not appear in Refs. [55,56,58] where the spatial dispersion was not taken into account.

For experimental observation of the predicted unstable plasmon mode in graphene with a drift current bias, the realization of necessary conditions for the hydrodynamic regime in graphene is mandatory. As discussed in the Introduction, such conditions can be fulfilled at temperatures higher than 30–100 K (depending on the carrier density in graphene) for frequencies below 5 THz. For utilizing the slow unstable plasmon mode in practice, special transducers for excitation of this mode and for conversion of the amplified mode into THz signal are needed.

In conclusion, we predict the existence of a slow plasmon mode in a single-layer graphene with a drift-current bias in the hydrodynamic regime. The mode disappears for zero carrier drift instead of transforming into any plasmon mode existing in graphene without carrier drift. We show that this mode becomes unstable in lossy hydrodynamic graphene with a drift-current bias and disappears in a lossless case. The instability appears even in a single-layer graphene and becomes stronger for greater losses in graphene in hydrodynamic regime. The dissipative instability occurs for any finite drift velocity but the instability increment decreases down to zero for vanishing carrier drift velocity. The strongest instability develops for codirected carrier drift and plasmon propagation directions. The instability increment decreases for oblique angles between the carrier drift and plasmon propagation directions so that the unstable mode becomes damped for angular deflection between those directions greater than 45° and finally this mode disappears in the case of transversal drift. These remarkable properties of predicted dissipative instability drastically differentiate it from the Cherenkov instability, which exists only in coupled plasmonic systems (with the carrier drift at least in one of them) even in a lossless case if the plasmon phase velocity is smaller than drift velocity, and it is prohibited in a single-layer graphene. For describing the plasmon dissipative instability, we extend the existing hydrodynamic theory by taking into account the effect of static biasing (drift-inducing) electric field on the oscillating hydrodynamic variables for arbitrary angle between the carrier drift and plasmon propagation directions. The results of this paper can be used for creating miniature amplifiers and emitters based on hydrodynamic graphene operating at room temperature in THz frequency range.

Financial support for this work was provided by the Russian Science Foundation (Project No. 22-79-00262).

[1] R. Pindak and D. Moncton, Two-dimensional systems, Phys. Today **35**(5), 57 (1982).

[2] F. Stern, Polarizability of a two-dimensional electron gas, Phys. Rev. Lett. **18**, 546 (1967).

[3] A. V. Chaplik, Possible crystallization of charge carriers in low-density inversion layers, Zh. Eksp. Teor. Fiz. **62**, 746 (1972) [Sov. Phys. JETP **35**, 395 (1972)].

[4] C. C. Grimes and G. Adams, Observation of two-dimensional plasmons and electron-ripplon scattering in a sheet of electrons on liquid helium, Phys. Rev. Lett. **36**, 145 (1976).

[5] S. J. Allen, Jr., D. C. Tsui, and R. A. Logan, Observation of the two-dimensional plasmon in silicon inversion layers, Phys. Rev. Lett. **38**, 980 (1977).

[6] T. N. Theis, J. P. Kotthaus, and P. J. Stiles, Two-dimensional magnetoplasmon in the silicon inversion layer, Solid State Commun. **24**, 273 (1977).

[7] K. S. Novoselov, A. K. Geim, S. V. Morozov, D. Jiang, Y. Zhang, S. V. Dubonos, I. V. Grigorieva, and A. A. Firsov, Electric field effect in atomically thin carbon films, Science **306**, 666 (2004).

[8] A. K. Geim and A. H. MacDonald, Graphene: Exploring carbon flatland, Phys. Today **60**(8), 35 (2007).

[9] P. Ajayan, P. Kim, and K. Banerjee, Two-dimensional van der Waals materials, Phys. Today **69**(9), 38 (2016).

[10] G. W. Hanson, Dyadic Green's functions and guided surface waves for a surface conductivity model of graphene, J. Appl. Phys. **103**, 064302 (2008).

[11] M. Jablan, H. Buljan, and M. Solace, Plasmonics in graphene at infrared frequencies, Phys. Rev. B **80**, 245435 (2009).

[12] F. H. L. Koppens, D. E. Chang, and F. J. G. Abajo, Graphene plasmonics: A platform for strong light–matter interactions, Nano Lett. **11**, 3370 (2011).

[13] Y. Li, K. Tantiwanichapan, A. K. Swan, and R. Paiella, Graphene plasmonic devices for terahertz optoelectronics, Nanophotonics **9**, 1901 (2020).

[14] J. A. Delgado-Notario, W. Knap, V. Clericò, J. Salvador-Sánchez, J. Calvo-Gallego, T. Taniguchi, K. Watanabe, T. Otsuji, V. V. Popov, D. V. Fateev *et al.*, Enhanced terahertz detection of multigate graphene nanostructures, Nanophotonics **11**, 519 (2022).

[15] D. A. Bandurin, D. Svintsov, I. Gayduchenko, S. G. Xu, A. Principi, M. Moskotin, I. Tretyakov, D. Yagodkin, S. Zhukov, T. Taniguchi *et al.*, Resonant terahertz detection using graphene plasmons, Nat. Commun. **9**, 5392 (2018).

[16] S. Chakraborty, O. P. Marshall, T. G. Folland, Y.-J. Kim, A. N. Grigorenko, and K. S. Novoselov, Applied optics. Gain modulation by graphene plasmons in aperiodic lattice lasers, Science **351**, 246 (2016).

[17] I. M. Moiseenko, V. V. Popov, and D. V. Fateev, Amplified propagating plasmon in asymmetrical graphene periodic structure, J. Phys. Commun. **4**, 071001 (2020).

[18] V. Ryzhii, T. Otsuji, and M. Shur, Graphene based plasma-wave devices for terahertz applications, Appl. Phys. Lett. **116**, 140501 (2020).

[19] M. Shur G. Aizin, T. Otsuji, and V. Ryzhii, Plasmonic field-effect transistors (TeraFETs) for 6G communications, Sensors **21**, 7907 (2021).

[20] B. N. Narozhny, Electronic hydrodynamics in graphene, Ann. Phys. (NY) **411**, 167979 (2019).

[21] A. Lucas and K. C. Fong, Hydrodynamics of electrons in graphene, J. Phys.: Condens. Matter **30**, 053001 (2018).

[22] S. Rudin, Non-linear plasma oscillations in semiconductor and graphene channels and application to the detection of terahertz signals, Int. J. High Speed Electron. Syst. **20**, 567 (2011).

[23] D. Svintsov, Hydrodynamic-to-ballistic crossover in Dirac materials, Phys. Rev. B **97**, 121405(R) (2018).

[24] D. Svintsov, V. Vyurkov, V. Ryzhii, and T. Otsuji, Hydrodynamic electron transport and nonlinear waves in graphene, Phys. Rev. B **88**, 245444 (2013).

[25] D. Bandurin, I. Torre, R. K. Kumar, M. B. Shalom, A. Tomadin, A. Principi, G. H. Auton, E. Khestanova, K. S. Novoselov, I. V. Grigorieva *et al.*, Negative local resistance caused by viscous electron backflow in graphene, Science **351**, 1055 (2016).

[26] C. Kumar, J. Birkbeck, J. A. Sulpizio, D. Perello, T. Taniguchi, K. Watanabe, O. Reuven, T. Scaffidi, A. Stern, A. K. Geim *et al.*, Imaging hydrodynamic electrons flowing without Landauer-Sharvin resistance, Nature (London) **609**, 276 (2022).

[27] D. A. Bandurin, A. V. Shytov, L. S. Levitov, R. K. Kumar, A. I. Berdyugin, M. B. Shalom, I. V. Grigorieva, A. K. Geim, and G. Falkovich, Fluidity onset in graphene, Nat. Commun. **9**, 4533 (2018).

[28] S. V. Morozov, K. S. Novoselov, M. I. Katsnelson, F. Schedin, D. C. Elias, J. A. Jaszczak, and A. K. Geim, Giant intrinsic carrier mobilities in graphene and its bilayer, Phys. Rev. Lett. **100**, 016602 (2008).

[29] M. Orlita, C. Faugeras, P. Plochocka, P. Neugebauer, G. Martinez, D. K. Maude, A.-L. Barra, M. Sprinkle, C. Berger, W. A. de Heer *et al.*, Approaching the Dirac point in high-mobility multilayer epitaxial graphene, Phys. Rev. Lett. **101**, 267601 (2008).

[30] R. Krishna Kumar, D. A. Bandurin, F. M. D. Pellegrino, Y. Cao, A. Principi, H. Guo, G. H. Auton, M. Ben Shalom, L. A. Ponomarenko, G. Falkovich *et al.*, Superballistic flow of viscous electron fluid through graphene constrictions, Nat. Phys. **13**, 1182 (2017).

[31] A. Tomadin and M. Polini, Theory of the plasma-wave photoresponse of a gated graphene sheet, Phys. Rev. B **88**, 205426 (2013).

[32] A. Lucas, Sound waves and resonances in electron-hole plasma, Phys. Rev. B **93**, 245153 (2016).

[33] R. S. Shishir and D. K. Ferry, Velocity saturation in intrinsic graphene, J. Phys.: Condens. Matter **21**, 344201 (2009).

[34] V. E. Dorgan, M.-H. Bae, and E. Pop, Mobility and saturation velocity in graphene on SiO_2, Appl. Phys. Lett. **97**, 082112 (2010).

[35] M. B. Lundeberg, Y. Gao, R. Asgari, C. Tan, B. Van Duppen, M. Autore, P. A.-González, A. Woessner, K. Watanabe, T. Taniguchi *et al.*, Tuning quantum nonlocal effects in graphene plasmonics, Science **357**, 187 (2017).

[36] M. Sabbaghi, H.-W. Lee, T. Stauber, and K. S. Kim, Drift-induced modifications to the dynamical polarization of graphene, Phys. Rev. B **92**, 195429 (2015).

[37] B. Van Duppen, A. Tomadin, A. N. Grigorenko, and M. Polini, Current-induced birefringent absorption and non-reciprocal plasmons in graphene, 2D Mater. **3**, 015011 (2016).

[38] T. A. Morgado and M. G. Silveirinha, Nonlocal effects and enhanced nonreciprocity in current-driven graphene systems, Phys. Rev. B **102**, 075102 (2020).

[39] D. Correas-Serrano and J. S. Gomez-Diaz, Nonreciprocal and collimated surface plasmons in drift-biased graphene metasurfaces, Phys. Rev. B **100**, 081410(R) (2019).
[40] T. A. Morgado and M. G. Silveirinha, Drift-induced unidirectional graphene plasmons, ACS Photon. **5**, 4253 (2018).
[41] K. Y. Bliokh, F. J. Rodríguez-Fortuño, A. Y. Bekshaev, Y. S. Kivshar, and F. Nori, Electric-current-induced unidirectional propagation of surface plasmon-polaritons, Opt. Lett. **43**, 963 (2018).
[42] T. Wenger, G. Viola, J. Kinaret, M. Fogelström, and P. Tassin, Current-controlled light scattering and asymmetric plasmon propagation in graphene, Phys. Rev. B **97**, 085419 (2018).
[43] Y. Dong, L. Xiong, I. Y. Phinney, Z. Sun, R. Jing, A. S. McLeod, S. Zhang, S. Liu, F. L. Ruta, H. Gao *et al.*, Fizeau drag in graphene plasmonics, Nature (London) **594**, 513 (2021).
[44] W. Zhao, S. Zhao, H. Li, S. Wang, S. Wang, M. I. B. Utama, S. Kahn, Y. Jiang, X. Xiao, S. Yoo *et al.*, Efficient Fizeau drag from Dirac electrons in monolayer graphene, Nature (London) **594**, 517 (2021).
[45] T. A. Morgado and M. G. Silveirinha, Negative Landau damping in bilayer graphene, Phys. Rev. Lett. **119**, 133901 (2017).
[46] T. A. Morgado and M. G. Silveirinha, Morgado and Silveirinha reply, Phys. Rev. Lett. **123**, 219402 (2019).
[47] D. Svintsov and V. Ryzhii, Comment on "Negative landau damping in bilayer graphene," Phys. Rev. Lett. **123**, 219401 (2019).
[48] D. Svintsov, Emission of plasmons by drifting Dirac electrons: A hallmark of hydrodynamic transport, Phys. Rev. B **100**, 195428 (2019).
[49] G. Gumbs, A. Iurov, D. Huang, and W. Pan, Tunable surface plasmon instability leading to emission of radiation, J. Appl. Phys. **118**, 054303 (2015).
[50] V. V. Korotyeyev and V. A. Kochelap, Plasma wave oscillations in a nonequilibrium two-dimensional electron gas: Electric field induced plasmon instability in the terahertz frequency range, Phys. Rev. B **101**, 235420 (2020).
[51] M. V. Krasheninnikov and A. V. Chaplik, Theory of electromagnetic excitation of two-dimensional plasma waves in multilayer superlattices, Zh. Eksp. Teor. Fiz. **79**, 555 (1980) [Sov. Phys. JETP **52**, 279 (1980)].
[52] I. V. Smetanin, A. Bouhelier, and A. V. Uskov, Coherent surface plasmon amplification through the dissipative instability of 2D direct current, Nanophotonics **8**, 135 (2019).
[53] S. Boubanga-Tombet, W. Knap, D. Yadav, A. Satou, D. B. But, V. V. Popov, I. V. Gorbenko, V. Kachorovskii, and T. Otsuji, Room-temperature amplification of terahertz radiation by grating-gate graphene structures, Phys. Rev. X **10**, 031004 (2020).
[54] A. Laturia, M. L. Van de Put, and W. G. Vandenberghe, Dielectric properties of hexagonal boron nitride and transition metal dichalcogenides: From monolayer to bulk, Npj 2D Mater. Appl. **2**, 6 (2018).
[55] I. M. Moiseenko, V. V. Popov, and D. V. Fateev, Terahertz plasmon amplification in a double-layer graphene structure with direct electric current in hydrodynamic regime, Phys. Rev. B **103**, 195430 (2021).
[56] I. M. Moiseenko, V. V. Popov, and D. V. Fateev, Terahertz transverse electric modes in graphene with DC current in hydrodynamic regime, J. Phys.: Condens. Matter **34**, 295301 (2022).
[57] S. A. Mikhailov and K. Ziegler, New electromagnetic mode in graphene, Phys. Rev. Lett. **99**, 016803 (2007).
[58] I. M. Moiseenko, V. V. Popov, and D. V. Fateev, Terahertz amplification and lasing by using transverse electric modes in a two-layer-graphene-dielectric waveguide structure with direct current, J. Phys.: Condens. Matter **35**, 255301 (2023).